Automated Evaluation of the α^5 Term of Lepton $g-2$: Progress Report

presented at

Loops and Legs in Quantum Field Theory 2006

Eisenach, Germany, April 23-28, 2006

Toichiro Kinoshita

Laboratory of Elementary-Particle Physics
Cornell University, Ithaca, New York U. S. A. 14853

in collaboration with

T. Aoyama, M. Hayakawa, and M. Nio

Theoretical Physics Laboratory, RIKEN
Wako, Saitama, Japan 351-0198

1. Introduction

- **This is a progress report of our work on the α^5 term of lepton $g-2$ which began more than two years ago.**
- **In this talk I will focus on the 10th-order diagrams that have no closed lepton loop (called *q-type*).**
- **These diagrams are extremely large and complicated and hardest to evaluate of all 10th-order diagrams.**
- **It would be practically impossible to evaluate them without highly automated algorithm.**
- **Initial reports on automation are given in**

T. Aoyama, M. Hayakawa, T. Kinoshita and M. Nio, Nucl. Phys. B 740, 138 (2006).

T. Aoyama, M. Hayakawa, T. Kinoshita and M. Nio, Nucl. Phys. B (Proc. Suppl.) xxx, yyy (2006).

T. Kinoshita, Nucl. Phys. B (Proc. Suppl.) xxx, yyy (2006).

2. Electron $g-2$: Measurement.

- **In 1987 the value of electron g-2 was improved over previous best value by three orders of magnitude in a Penning trap experiment by Dehmelt et al. at U. of Washington.**

Van Dyck *et al.*, **PRL 59, 26 (1987)**

- **Their final results were:**

$$\mathbf{a_{e^-} = 1\ 159\ 652\ 188.4\ (4.3) \times\ 10^{-12}}$$

$$\mathbf{a_{e^+} = 1\ 159\ 652\ 187.9\ (4.3) \times\ 10^{-12}}$$

- **Reanalysis of these data and their combination assuming CPT invariance leads to**

$$\mathbf{a_e[UW87] = 1\ 159\ 652\ 188.3\ (4.2) \times\ 10^{-12}}$$

Mohr and Taylor, RMP 77, 1 (2005)

- **Measurement uncertainty was dominated by cavity shift due to interaction of electron with hyperboloid cavity which has complicated resonance structure.**

- **Several ways to reduce this error examined:**

(a) Use cavity with smaller Q.

van Dyck, et al., 1991, unpublished.

(b) Study cavity shift of many ($\sim$ 1000)-electron cluster.

Mittleman, et al., PRL 75, 2839 (1995)

(c) Use cylindrical cavity, whose property is known analytically.

Brown, Gabrielse, RMP 58, 233 (1986)

- **Gabrielse's new measurement of a_e is based on (c).**
  - **A preliminary result was reported:**

$$\mathbf{a_{e^-}[HV05] = 1\ 159\ 652\ 180.86\ (0.57) \times 10^{-12} \qquad (0.49\ ppb)}$$

B. Odom, PhD thesis, Harvard University, 2005

  - **7.5 times more precise than the Seattle result.**
  - **Another set of measurements has just been finished.**
  - **The new result ?**

3. Theory of Electron $g-2$ up to Order α^4

$$\mathbf{a_e(QED) = A_1 + A_2(m_e/m_\mu) + A_2(m_e/m_\tau) + A_3(m_e/m_\mu, m_e/m_\tau)}$$

$$\mathbf{A_i = A_i^{(2)}\left(\frac{\alpha}{\pi}\right) + A_i^{(4)}\left(\frac{\alpha}{\pi}\right)^2 + A_i^{(6)}\left(\frac{\alpha}{\pi}\right)^3 + \ldots,\ i = 1, 2, 3}$$

$\mathbf{A_1^{(2)} = 0.5}$ **1 diagram (analytic)**

$\mathbf{A_1^{(4)} = -0.328\,478\,965\ \ldots}$ **7 diagrams (analytic)**

$\mathbf{A_1^{(6)} = 1.181\,241\,456\ \ldots}$ **72 diagrams (numerical, analytic)**

Kinoshita, PRL 75, 4728 (1995)

Laporta, Remiddi, PLB 379, 283 (1996)

$\mathbf{A_1^{(8)} = -1.728\,3\,(35)}$ **891 diagrams (numerical)**

Kinoshita, Nio, Phys. Rev. D 73, 013003 (2006)

- **Error of $A_1^{(8)}$ reduced to one-tenth of old one.**
- $\mathbf{A_2}$ **term is small** $:\sim \mathbf{2.72 \times 10^{-12}}$.
- $\mathbf{A_3}$ **term is even smaller** $:\sim \mathbf{2.4 \times 10^{-21}}$.
- **Non – QED term (Standard Model) is small, too** : $\mathbf{1.70(2) \times 10^{-12}}$.
- **This is why a_e provides a very good test of QED.**

- **To compare theory with measurement we need α.**
- **At present best α available are**

$$\alpha^{-1}(\mathbf{h}/M_{Rb}) = \mathbf{137.035\ 998\ 78\ (91)} \qquad [\mathbf{6.7\ ppb}]$$

P. Cladé et al., PRL 96, 033001 (2006)

$$\alpha^{-1}(\mathbf{h}/M_{Cs}) = \mathbf{137.036\ 000\ 1\ (11)} \qquad [\mathbf{7.7\ ppb}]$$

Wicht, Hensley, Sarajlic, Chu, Physica Scripta T102, 82-88 (2002)

- **Assuming $\mathbf{A_1^{(10)}} = \mathbf{0.0(3.8)}$ (pure guess by Mohr-Taylor) we obtain**

$$\mathbf{a_e}(\mathbf{h}/\mathbf{M_{Rb}}) = \mathbf{1\ 159\ 652\ 188.70}\ (\mathbf{0.10})(\mathbf{0.26})(\mathbf{7.71}) \times\ \mathbf{10^{-12}}$$

$$\mathbf{a_e}(\mathbf{h}/\mathbf{M_{Cs}}) = \mathbf{1\ 159\ 652\ 177.55}\ (\mathbf{0.10})(\mathbf{0.26})(\mathbf{9.32}) \times\ \mathbf{10^{-12}}$$

$$(\mathbf{8th})(\mathbf{10th})(\alpha(h/M))$$

and

$$\mathbf{a_e}[\mathbf{HV05}] - \mathbf{a_e}(\mathbf{h}/\mathbf{M_{Rb}}) = -\mathbf{7.8}\ (\mathbf{7.8}) \times\ \mathbf{10^{-12}}$$

$$\mathbf{a_e}[\mathbf{HV05}] - \mathbf{a_e}(\mathbf{h}/\mathbf{M_{Cs}}) = \quad \mathbf{3.3}\ (\mathbf{9.4}) \times\ \mathbf{10^{-12}}$$

- **Striking feature of $a_e(h/M_{Rb})$ and $a_e(h/M_{Cs})$ is that their errors come predominantly from measurements of α.**

- **This means that non-QED α, even the best ones, is too crude to test QED to the extent made possible by the progress of theory and measurement of a_e.**

- **Instead we can turn the argument around and calculate α assuming that QED is still valid.**

- **This yields very precise values:**

$$\alpha^{-1}(a_e[UW87]) = \mathbf{137.035\ 998\ 834\ (12)(31)(502)\quad [3.7\ ppb]}$$

$$\alpha^{-1}(a_e[HV05]) = \mathbf{137.035\ 999\ 708\ (12)(31)(68)\quad [0.55\ ppb]}$$

- **Fig. 1 gives graphic comparison of some α's.**

- **To show finer details of lower half the horizontal scale is enlarged by 10 in Fig. 2.**

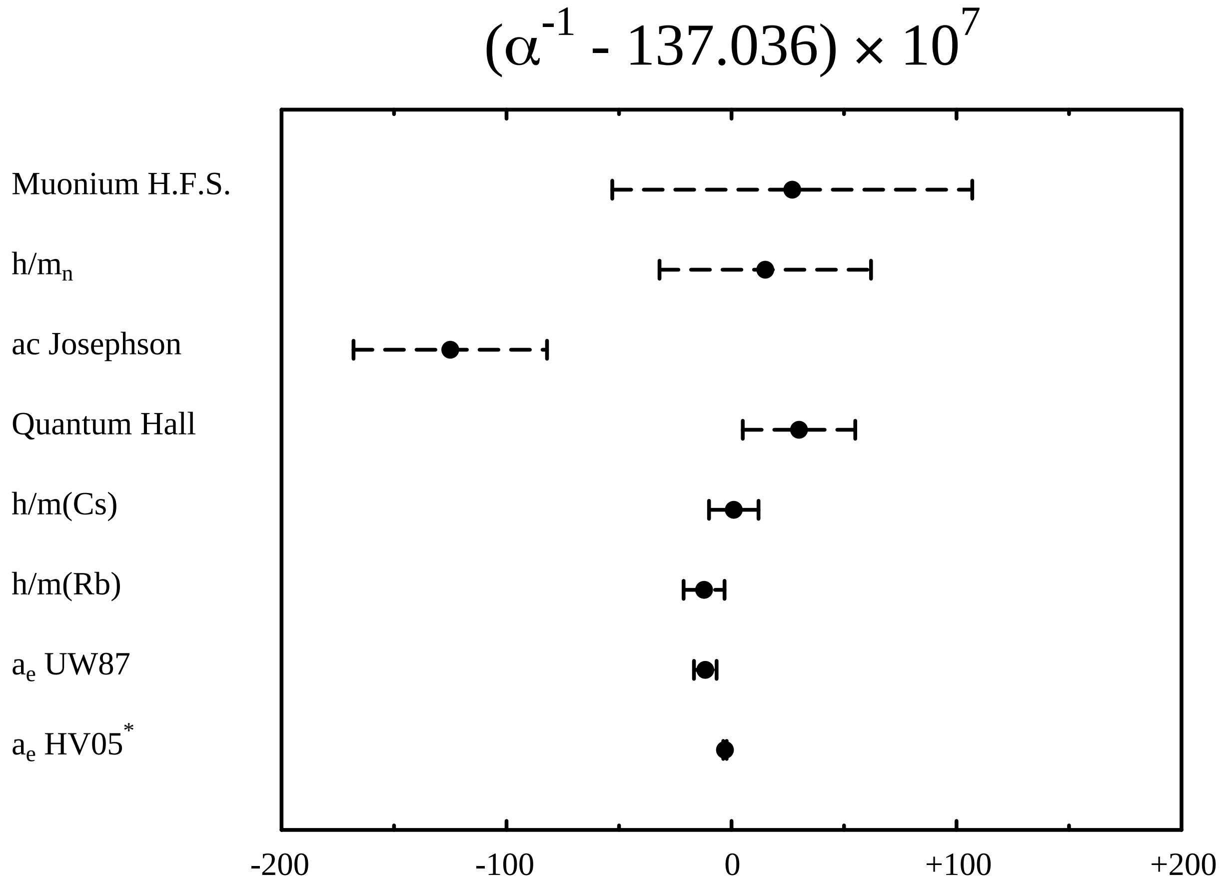

Figure 1: **Comparison of various α^{-1}. $\alpha(h/m_{Cs})$ may be improved by factor 2. The superscript * on a_eHV05* means that the corresponding α is still tentative.**

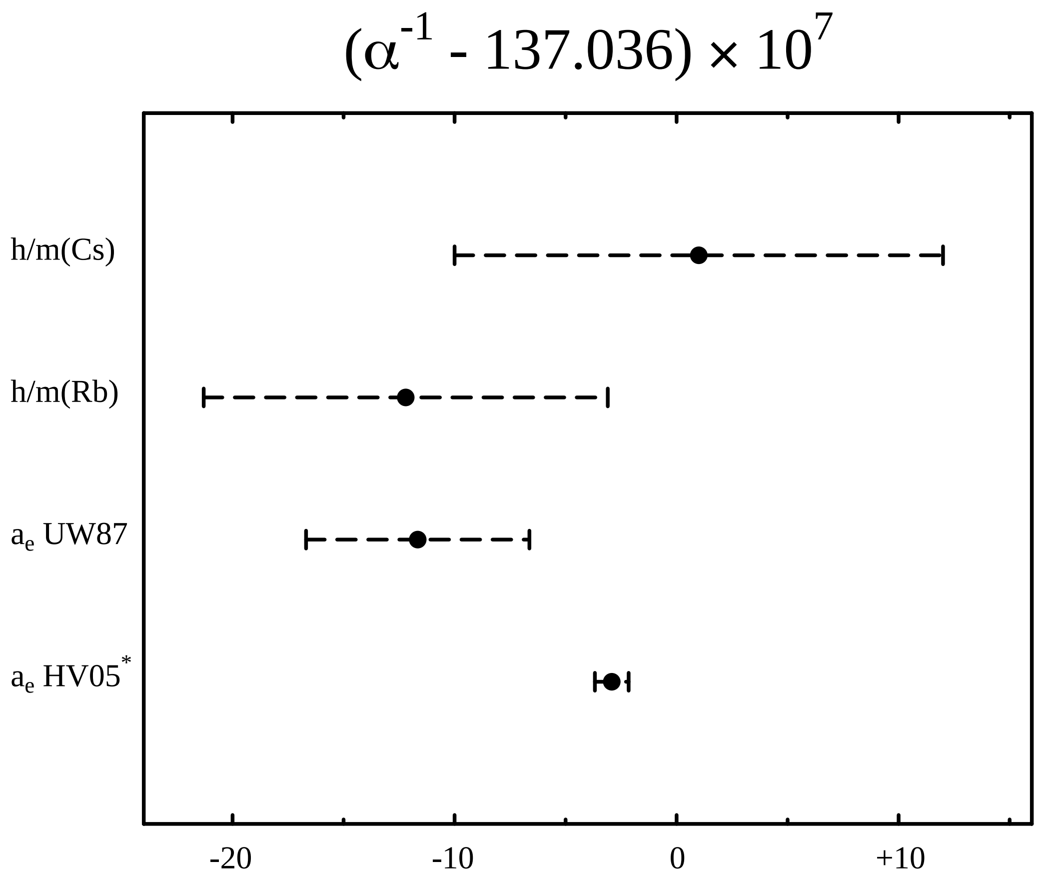

Figure 2: **Magnification of the lower half of Fig. 4 by factor 10.**

4. Tenth-order term: Why needed ?

- **Uncertainty in $\alpha(a_e$[HV05]$)$ is only factor 2 larger than that of theory, which is mostly from the α^5 term.**
- **Thus, when measurement improves by just factor 2, an actual value of α^5 term becomes necessary to improve $\alpha(a_e)$ further.**
- **This is why the α^5 term deserves serious investigation.**
- **12672 Feynman diagrams contribute to the α^5 term.**
- **Real challenge to tackle such a gigantic problem.**
- **First step:**
  Classify all diagrams into gauge-invariant sets.
- **There are 32 g-i sets within 6 supersets as shown next.**

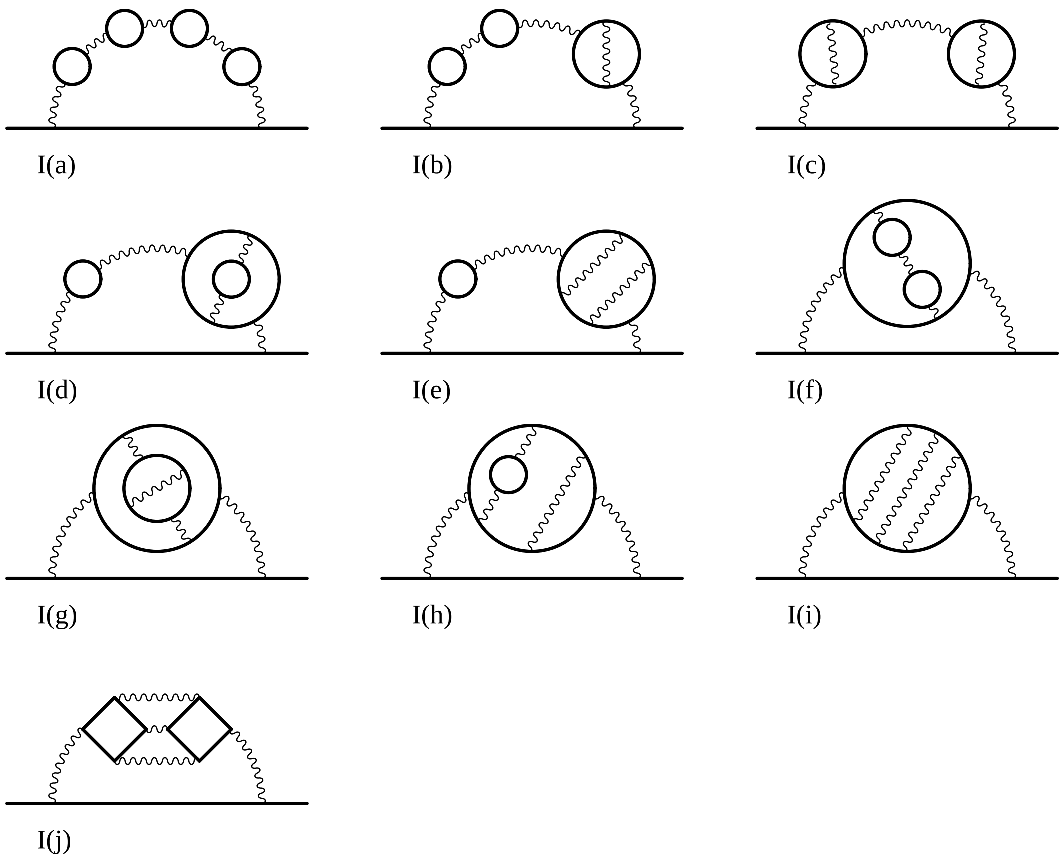

Figure 3: **Self-energy-like diagrams representing 208 vertex dgrms of set I.**

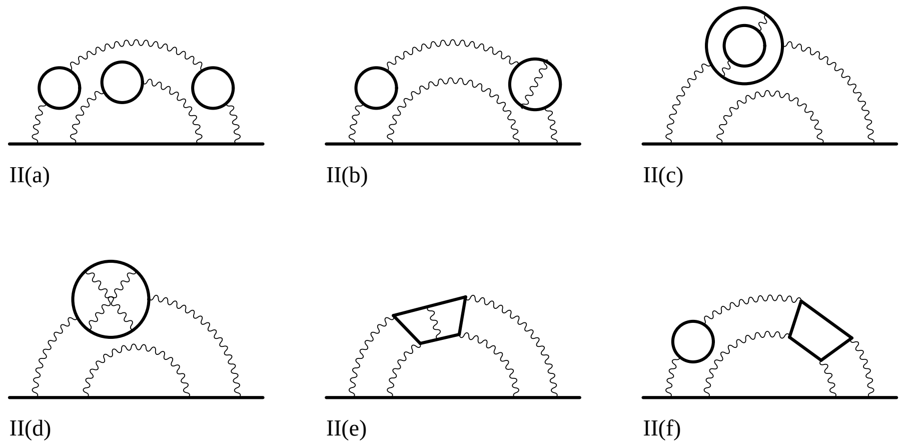

Figure 4: **Diagrams of Set II which consists of 600 vertex diagrams.**

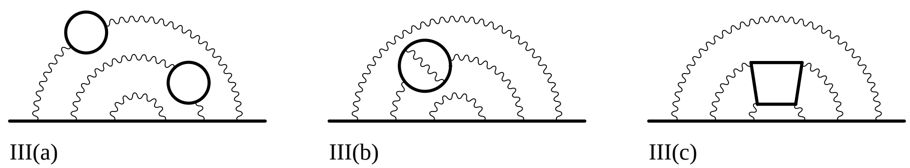

Figure 5: **Diagrams of Set III which consists of 1140 vertex diagrams.**

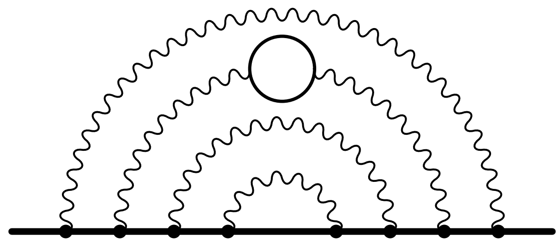

Figure 6: **Diagrams of Set IV which consists of 2072 vertex diagrams.**

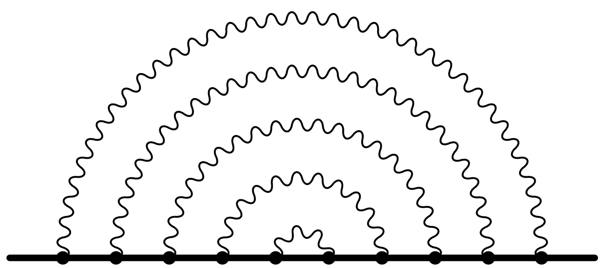

Figure 7: **Diagrams of Set V which consists of 6354 vertex diagrams.**

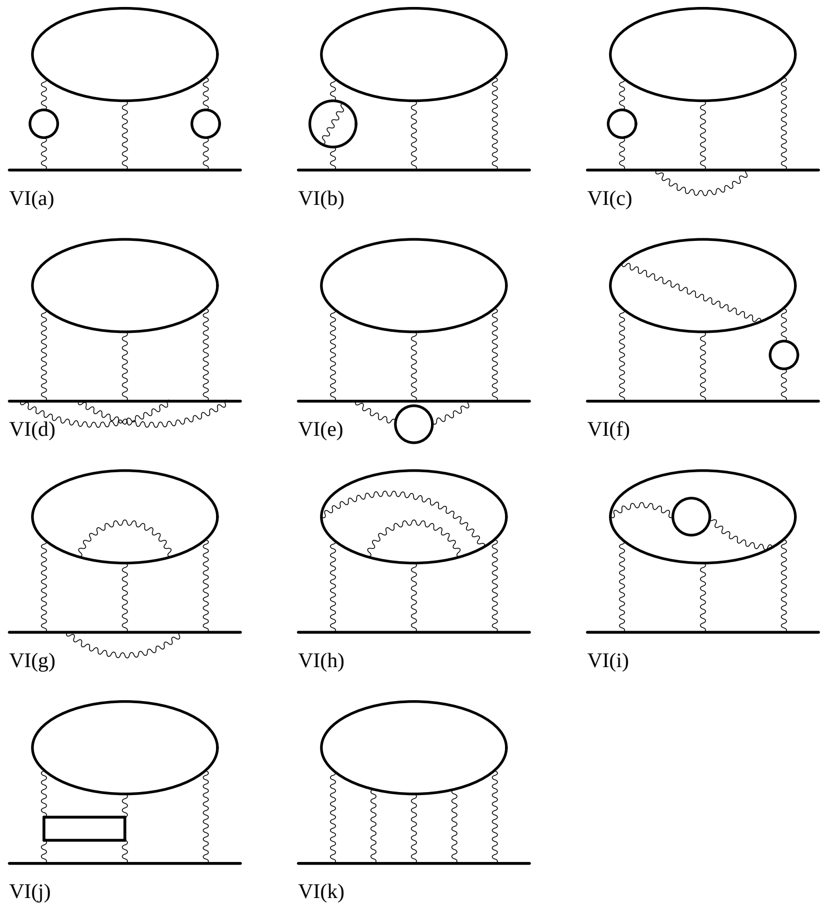

Figure 8: **Diagrams of Set VI which consists of 2298 vertex diagrams.**

- **Largest and most difficult is the Set V, which consists of 6354 Feynman diagrams of "q-type".**
- **We are thus focused on Set V since others, being less complicated, are easier to handle.**
- **Set V has a simplifying feature that sum of nine vertex diagrams can be related to one self-energy diagram by**

$$\mathbf{\Lambda}^{\nu}(\mathbf{p},\mathbf{q}) \simeq -\mathbf{q}_{\mu}\left[\frac{\partial \mathbf{\Lambda}_{\mu}(\mathbf{p},\mathbf{q})}{\partial \mathbf{q}_{\nu}}\right]_{\mathbf{q}=\mathbf{0}} - \frac{\partial \mathbf{\Sigma}(\mathbf{p})}{\partial \mathbf{p}_{\nu}}$$

derived from the Ward-Takahashi identity.

- **This enables us to reduce number of diagrams to 706.**
- **Time-reversal invariance reduces it further to 389 shown in the next page.**

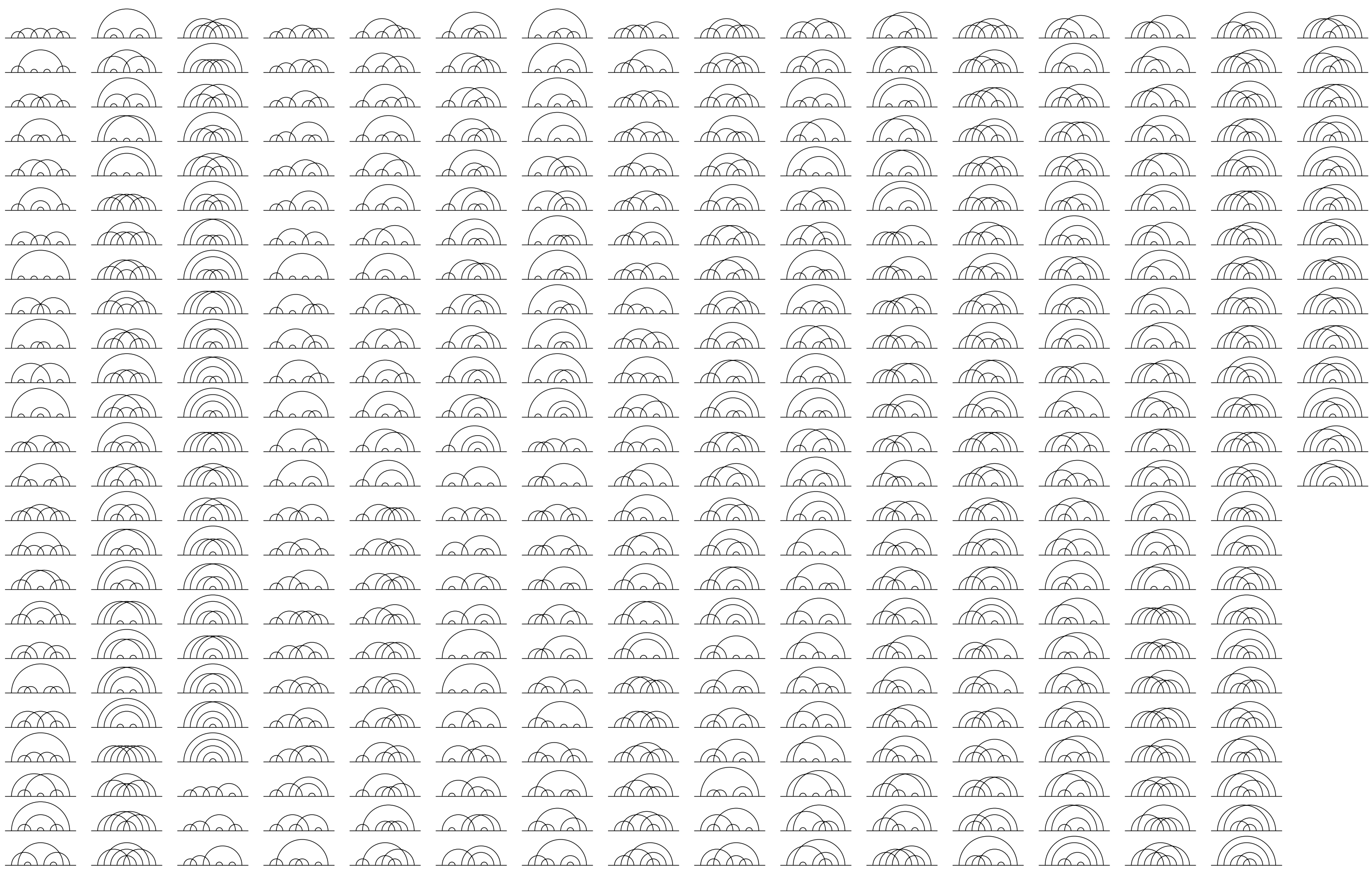

Figure 9: **Overview of all diagrams contributing to Set V.**

- **Analytic integration is likely to be far in the future.**
- **Numerical integration is the only viable option at present.**
- **Fortunately, algebraic part of manipulation developed for α^3 case and extended for α^4 applies to α^5, too.**
- **For α^5, however, every step must be fully automated.**
- **Also, master code is needed to run all steps automatically.**
- **Let us now sketch these steps.**

- **Step I: Diagram generation**

  - **Each (q-type) diagram is expressed by a single-line code which specifies pattern of pairing of vertices by photon propagators.**

  - **Algorith implemented by C++.**

  - **Diagrams are named X001,..., X389 and stored as plain-text file.**

  - **This file enables us to identify all UV divergent subdiagrams according to certain algorithm.**

  - **Implemented by both Perl and C++.**

  - **Step I is crucial for automatic control of all subsequent steps.**

  - **It was not needed in α^3 and α^4 cases which were simple enough to go without it.**

- **Step II: Construct unrenormalized integrand**

  - **Translate one-line rep. of diagram into integrand.**

  - **Carry out momentum integration analytically and express result as integral over Feynman parameters $z_1, z_2, \cdots, z_N$, and "symbols" B_{ij}, A_i, U, V :**

$$\int (dz)_G J_G,$$

  where

$$(dz)_G \equiv \prod_{i=1}^{N} dz_i \delta(1 - \sum_{i=1}^{N} z_i), \qquad J_G = \frac{F_0(B_{ij}, A_i)}{U^2 V^{n-1}} + \frac{F_1(B_{ij}, A_i)}{U^3 V^{n-2}} + \cdots .$$

  - **Previously J_G was obtained by FORM using home-made integration table written in FORM.**

  - **Now automation of Step II proceeds as follows:**

    Diagram info. → input for FORM, obtained by Perl

    → analytic integration using integration table in FORM.

- **Step III: Construct building blocks**
  - **Get $B_{ij}, C_{i,j}, A_i, U, V$ as homog. polynomials of $z_1, z_2, \ldots, z_N$.**
    - $\star$ **U, B_{ij} are related to loop momenta, and determined by the topology of diagram.**
    - $\star$ **A_i are related to flow of external momenta, and satisfy Kirchhoff"s laws for "currents".**
  - **Easy to obtain B_{ij}, U, etc. by hand in 6th- and 8th-orders. Much harder in 10th-order.**
  - **We now calculate them automatically:**

    input info. $\rightarrow B_{ij}, C_{i,j}, U, \ldots$ by MAPLE and FORM.
  - **They are also derived in C++.**
  - **V has form common to all diagrams:**

$$V = \sum_{i}^{electrons} z_i(1 - A_i) + \sum_{i}^{photons} z_i \lambda^2,$$

where electron mass is put to one and λ is infrared cutoff.

- **Step IV: Construct UV subtraction terms**
  - **Most difficult part is renormalization.**
  - **Textbook renormalization is not suitable for putting on computer and known only to lowest order anyway.**
  - **We start from subtractive regularization.**
  - **Subtraction integrand is derived from original integrand by applying K-operation, defined for each divergent subdiagram based on simple power-counting rule.**
  - **Properties of K-operation:**
    - ⋆ **Subtraction of UV divergence is pointwise.**
    - ⋆ **It is built so that it factorize analytically into product of lower-order quantities, an important feature for cross-checking with other diagrams.**
    - ⋆ **It contains only UV-divergent part of renormalization constant. Thus additional (finite) renormalization is required.**

- **This subtraction scheme applied to all subdiagram divergences regularizes the original integral, yielding**

$$\Delta M_G = M_G - \sum_{f\in\mathcal{F}} X_f$$

$$= \int (dz)_G [J_G - \sum_{f\in\mathcal{F}} K_f J_G]$$

where $\mathcal{F}$ is the set of Zimmermann's forest f of divergent subdiagrams.

- **IR-divergence can be handled similarly by IR power-counting rule.**

- **These procedures had been developed for α^3 and α^4 cases by partly-automatic means using FORM.**

- **Now they are fully automated:**

  input info. $\rightarrow$ subtraction terms in FORTRAN

  implemented by Perl with help by MAPLE and FORM.

• Step V: Residual renormalization

- **Output of Steps I - IV are UV- (and IR-) finite integral.**
- **However, it is not standard renormalized amplitude (although it is on-shell).**
- **Finite residual renormalization must be carried out to get observable g-2.**
- **Residual renormalization was easy for α^3 case and still manageable by hand for α^4.**
- **For α^5, however, number of UV subtraction terms (each being integral of up to 8th-order) is 13150 so that summing up residual renormalization terms becomes a huge operation.**
- **Number of IR subtraction terms is large, too.**
- **Thus Step V must be fully automated, achieved by Perl, MAPLE, and FORM.**

- **Controling whole steps:**
  - **Each step of code generation is achieved by individual Perl program helped by MAPLE and FORM.**
  - **Flow of entire process governed by shell script.**
  - **It takes the name of diagrams (X001,...,X389) as input and performs following operations:**

    (a) Find the input information from data file prepared in Step I.

    (b) Construct components of integration code in FORTRAN.

    (c) Gather all FORTRAN codes in the end.
  - **Step V can be attached at the end of Step IV to make the entire process automatic.**
  - **But we are treating Step V separately for the moment.**

- **Thus far we completed Steps I, II, III, IV for 135 diagrams which have only UV-divergent vertex subdiagrams.**

- **For 254 diagrams containing self-energy subdiagrams Steps I - III have been completed.**

- **But Step IV requires more work because these diagrams have also logarithmic IR divergence and, in some cases, linear IR-divergence.**

- **Linear IR divergence is caused by our approach which splits selfmass counterterm into UV-div. and UV-finite parts and subtracts UV-divergent part only:**

$$\cdots \frac{1}{\not{p}-m} \left((\delta m - \delta m^{UV}) + B(\not{p}-m)\right)\frac{1}{\not{p}-m}\cdots$$

- **In second order case we have $\delta m - \delta m^{UV} = 0$.**

- **However, $\delta m - \delta m^{UV} \neq 0$ in other cases, which causes an extra pole in the IR limit.**

- **While waiting for full automation code, we decided to deal with IR problem temporarily by giving a finite cutoff to photon mass.**

- **To obtain better result for numerical integration it is important to subtract linear IR pole explicitly.**

- **At present this is done by hand, but is being automated.**

- **Once linear divergence is removed, logarithmic divergence can be handled easily by photon mass cutoff.**

- **As warm-up, we have tested this approach for sixth-order and eighth-order cases.**

- α^3 **case:**

q-type only	**Photon cutoff** $\lambda^2 = 10^{-6}$	**Exact treatment**
	0.8941 (272)	**0.904979...**

  - ⋆ **All diagrams generated in 39 seconds on DEC** α**.**
  - ⋆ 10^7 **sampling points 50 iterations took 25 - 45 min on DEC** α**.**

- **Effect of cutoff seems to be within errorbars.**

- **Good agreement shows that our automating algorithm is bug-free and gives good approximate answer.**

- α^4 **case:**

q-type only	**cutoff** $\lambda^2 = 10^{-4}$	**numerical with** $\lambda = 0$
	-2.1005 (1216)	**-1.9931 (35)**

  - $\star$ **All 47 diagrams generated in 1240 seconds on DEC** α**.**
  - $\star$ 10^7 **sampling points 50 iterations using 64 CPU took 8 min to 100 min.**
  - $\star$ **Final results required up to 150 iterations.**

- **Good agreement provides the confirmation of previous eighth-order code.**

- **This is the first independent check of the eighth-order code.**

- **Current status of numerical integration:**

  - **Crude evaluation by VEGAS of all 389 integrals has been carried out.**

  - **Table 1 lists all diagrams with only vertex renormalization terms. Photon mass is set equal to 0.**

  - **Tables 2 and 3 list diagrams with at least one self-energy renormalization terms, evaluated with photon mass set equal to** $10^{-2}m_e$**.**

Table 1: 135 diagrams which have at the vertex corrections only. Phton mass is set to be zero.

X001	47	-0.2981	0.0327	X003	19	-0.1142	0.0094	X013	7	-1.3540	0.0038	X014	31	0.7833	0.0141
X015	2	2.1020	0.0019	X016	2	-0.9609	0.0019	X019	31	1.2183	0.0140	X021	11	-0.2967	0.0049
X031	2	2.2932	0.0029	X032	2	-0.2426	0.0013	X033	2	-1.3771	0.0014	X034	2	1.2539	0.0021
X035	2	-0.5838	0.0014	X037	2	-0.7416	0.0020	X039	11	0.3164	0.0044	X047	2	-4.4551	0.0033
X048	2	-0.8051	0.0016	X049	2	-0.0295	0.0013	X050	2	-1.2222	0.0018	X051	2	-0.1733	0.0020
X053	2	0.3646	0.0015	X055	2	-0.3634	0.0014	X076	19	-5.2424	0.0230	X077	39	3.2616	0.0443
X078	39	0.9403	0.0453	X091	39	-1.8168	0.0486	X093	7	-1.7604	0.0050	X094	15	-1.0460	0.0099
X095	7	0.5791	0.0043	X096	31	1.2849	0.0179	X101	15	-0.2625	0.0093	X102	31	-1.3912	0.0312
X103	31	0.8229	0.0193	X115	7	-0.5947	0.0065	X116	7	1.8059	0.0050	X117	7	0.3232	0.0045
X118	15	-3.2225	0.0106	X119	15	-0.1055	0.0113	X120	31	1.7913	0.0158	X121	7	-0.8630	0.0044
X122	7	-0.7414	0.0042	X123	15	-3.3339	0.0075	X125	31	0.7481	0.0189	X127	15	1.1349	0.0059
X128	31	0.5916	0.0129	X129	31	1.4312	0.0123	X165	15	-2.1380	0.0114	X166	15	-2.2856	0.0121
X172	31	1.4301	0.0225	X178	5	0.7079	0.0038	X179	2	-0.4378	0.0034	X180	11	0.0242	0.0044
X185	5	-0.1313	0.0050	X186	23	1.1634	0.0049	X195	2	-1.0665	0.0045	X196	2	-2.0375	0.0029
X197	2	-0.3870	0.0022	X198	5	-2.3452	0.0027	X199	5	1.0493	0.0038	X200	11	0.0092	0.0042
X201	2	-0.4877	0.0037	X202	2	1.9243	0.0030	X203	2	0.9037	0.0023	X204	11	-1.9324	0.0038
X205	5	-0.9038	0.0049	X206	23	1.6447	0.0065	X207	5	0.2894	0.0042	X208	11	0.5215	0.0040
X209	5	0.1444	0.0040	X210	23	0.7653	0.0049	X225	23	0.2928	0.0098	X231	11	-0.7467	0.0058
X232	23	0.4010	0.0116	X235	23	0.7040	0.0100	X259	5	0.0160	0.0049	X260	5	-0.4007	0.0036
X265	5	-0.6741	0.0034	X266	11	0.1179	0.0048	X271	11	0.2415	0.0053	X272	23	-0.7339	0.0093
X275	2	-0.7434	0.0045	X276	2	-0.5545	0.0028	X277	2	2.7843	0.0015	X278	5	-0.1559	0.0044
X279	5	0.8231	0.0038	X280	2	-1.0096	0.0046	X281	5	-1.3724	0.0041	X282	5	0.4841	0.0034
X283	11	-0.0505	0.0042	X284	2	-0.2711	0.0032	X285	5	0.0169	0.0039	X286	11	0.7775	0.0038
X287	23	0.1874	0.0068	X296	5	0.5448	0.0046	X297	5	-0.4792	0.0047	X303	2	0.3213	0.0025
X304	5	-0.3422	0.0049	X305	5	0.4619	0.0040	X313	11	0.9513	0.0043	X314	23	0.7992	0.0070
X320	11	0.5585	0.0045	X321	23	-0.9154	0.0078	X322	23	0.9205	0.0032	X343	2	3.8805	0.0029
X344	2	3.4147	0.0037	X345	2	-1.0015	0.0024	X346	2	0.2844	0.0037	X347	2	-2.6792	0.0028
X348	2	-0.4859	0.0038	X349	5	2.0816	0.0043	X350	2	1.4548	0.0023	X351	5	0.2449	0.0034
X352	2	-0.1319	0.0025	X353	5	0.1884	0.0025	X354	5	-2.0375	0.0025	X355	11	-1.0637	0.0031
X356	5	2.0708	0.0049	X357	5	0.3634	0.0037	X358	5	0.0332	0.0042	X359	11	-0.1515	0.0046
X360	11	-0.4709	0.0042	X361	23	2.5319	0.0064	X362	2	-0.5660	0.0036	X363	2	-2.3416	0.0022
X364	2	2.3900	0.0021	X367	5	-0.7180	0.0049	X370	5	-1.4791	0.0045	X371	5	-0.0074	0.0042
X372	11	-1.2875	0.0025	X373	23	0.5684	0.0039	X376	5	1.0369	0.0034	X377	11	0.4192	0.0036
X378	11	1.3082	0.0034	X379	23	-0.3402	0.0052	X381	23	1.0677	0.0038				

Table 2: diagrams which have at least one self-energy diagrams as a subdiagram. Phton mass is set to be $10^{-2}m_e$.

X002	31	-33.9820	0.1052	X004	47	-2.3118	0.0458	X005	39	3.5780	0.0220	X006	31	35.4529	0.1246
X007	31	-19.3318	0.0601	X008	15	-125.3216	0.2421	X009	11	-6.1573	0.0293	X010	23	4.6521	0.2299
X011	23	28.2746	0.1214	X012	15	465.3961	1.0710	X017	5	0.4079	0.0048	X018	5	0.5155	0.0053
X020	35	-0.2799	0.1400	X022	39	0.1790	0.0048	X023	23	0.9465	0.0105	X024	31	0.6635	0.0258
X025	31	-5.3173	0.0256	X026	15	-587.1377	1.2820	X027	11	-4.3023	0.0166	X028	23	-11.7051	0.0312
X029	23	17.0434	0.0430	X030	15	18.8327	0.1307	X036	5	2.1506	0.0030	X038	5	-0.9682	0.0022
X040	23	0.5362	0.0036	X041	47	1.9855	0.0046	X042	31	3.1772	0.0066	X043	11	-2.3724	0.0124
X044	23	-8.8044	0.0232	X045	23	-0.2881	0.0294	X046	15	-8.9793	0.0909	X052	5	-5.7255	0.0081
X054	5	2.5318	0.0025	X056	5	-1.8669	0.0028	X057	17	-1.0600	0.0047	X058	11	-4.8284	0.0063
X059	17	1.6964	0.0040	X060	35	3.6874	0.0060	X061	35	2.6364	0.0084	X062	23	-0.6353	0.0133
X063	5	2.3682	0.0079	X064	5	0.1314	0.0060	X065	5	0.1766	0.0052	X066	11	4.5730	0.0120
X067	35	0.8282	0.0112	X068	23	4.4112	0.0123	X069	11	2.3579	0.0088	X070	23	6.8804	0.0174
X071	23	2.0306	0.0220	X072	15	0.4432	0.0439	X073	39	16.4023	0.0752	X074	39	21.2656	0.0737
X075	31	-52.8861	0.2211	X079	47	-2.4794	0.1004	X080	39	6.3429	0.0408	X081	31	38.9858	0.2133
X082	31	-50.9633	0.1835	X083	23	136.0695	0.4597	X084	15	10.9480	0.0359	X085	31	8.0807	0.0500
X086	31	11.1642	0.0406	X087	35	-0.5154	0.2684	X088	31	-29.2579	0.1473	X089	23	-365.8571	0.9782
X090	15	5.2876	0.0470	X092	31	8.7444	0.0435	X097	15	4.3940	0.0259	X098	31	0.2886	0.0190
X099	31	8.0924	0.0526	X100	35	-0.6524	0.2547	X104	47	5.1315	0.0366	X105	31	4.9794	0.0372
X106	35	17.6100	0.0920	X107	31	-24.2167	0.1383	X108	23	-355.2919	0.9930	X109	15	1.0280	0.0226
X110	31	4.0436	0.0294	X111	31	4.8049	0.0207	X112	35	17.3563	0.1231	X113	31	-16.7136	0.0789
X114	23	-29.3829	0.3151	X124	17	-12.3978	0.0386	X126	35	5.9229	0.0350	X130	35	5.9115	0.0264
X131	47	-0.1667	0.0363	X132	35	10.9981	0.0823	X133	15	2.6032	0.0226	X134	31	1.0672	0.0185
X135	31	1.9125	0.0213	X136	35	10.4033	0.0764	X137	31	11.5523	0.0764	X138	23	25.8442	0.2066
X139	23	99.1386	0.3072	X140	31	4.3251	0.0277	X141	35	-7.0427	0.2114	X142	31	-17.7118	0.0789
X143	23	-195.7388	0.5629	X144	23	9.3855	0.5761	X145	15	929.8793	2.3470	X146	23	-20.0316	0.0750
X147	11	2.0161	0.0135	X148	23	1.9408	0.0161	X149	11	-11.1951	0.0424	X150	23	-5.4652	0.0316
X151	31	15.0203	0.1025	X152	23	-85.7328	0.2294	X153	23	-85.8868	0.2188	X154	15	-46.4777	0.7341
X155	11	4.1684	0.0107	X156	23	3.1170	0.0141	X157	11	-21.8604	0.0753	X158	23	31.6657	0.0711
X159	23	31.5837	0.0594	X160	23	-122.0564	0.2747	X161	23	31.7185	0.1918	X162	15	-225.8251	0.7195
X163	15	8.0473	0.0369	X164	11	-21.1957	0.1058	X167	17	3.9551	0.0526	X168	15	2.8872	0.0232
X169	11	34.6371	0.1479	X170	31	5.5015	0.0426	X171	23	-30.9698	0.1136	X173	35	-3.9492	0.0519
X174	31	4.5300	0.0255	X175	23	22.2731	0.1129	X176	5	0.9735	0.0168	X177	11	1.8449	0.0237
X181	5	-3.0563	0.0117	X182	11	1.9156	0.0082	X183	5	2.4473	0.0164	X184	23	6.0180	0.0217
X187	5	1.6021	0.0098	X188	23	2.3760	0.0086	X189	11	-6.8526	0.0697	X190	23	-12.6108	0.0615
X191	11	0.6596	0.0140	X192	23	2.8687	0.0160	X193	11	-6.3484	0.0579	X194	23	-4.6499	0.0423

Table 3: diagrams which have at least one self-energy diagrams as a subdiagram. Phton mass is set to be $10^{-2}m_e$.

X211	17	3.1841	0.0150	X212	35	-1.1120	0.0164	X213	5	-2.4731	0.0138	X214	11	0.6360	0.0092
X215	5	0.4671	0.0119	X216	23	-0.4904	0.0092	X217	11	6.8885	0.0383	X218	23	0.4525	0.0292
X219	23	-24.8150	0.1232	X220	35	-3.9293	0.0650	X221	31	3.8682	0.0258	X222	23	10.4062	0.1213
X223	23	64.7598	1.0760	X224	23	5.0092	0.0269	X226	11	1.4026	0.0132	X227	23	0.9139	0.0102
X228	31	4.0965	0.0253	X229	23	-12.2259	0.0667	X230	23	-17.1385	0.1040	X233	15	-1.2406	0.0087
X234	31	2.1198	0.0122	X236	31	0.9006	0.0081	X237	35	4.3510	0.0318	X238	23	1.3740	0.0106
X239	31	-2.7690	0.0253	X240	23	19.1264	0.0818	X241	23	69.1008	0.1873	X242	35	-2.2962	0.0969
X243	23	-124.1828	0.2690	X244	23	-17.1150	0.0547	X245	23	1.9927	0.0101	X246	23	-4.8722	0.0267
X247	23	46.2950	0.1284	X248	23	-8.1875	0.0359	X249	11	2.9287	0.0083	X250	23	0.6967	0.0122
X251	23	0.0271	0.0083	X252	35	-8.4378	0.0548	X253	23	-4.9590	0.1141	X254	23	-0.4380	0.0229
X255	23	-45.7515	0.1178	X256	15	-52.4348	0.2768	X257	5	2.5577	0.0247	X258	5	0.5495	0.0124
X261	5	5.7366	0.0157	X262	5	-2.7083	0.0099	X263	5	-0.7775	0.0123	X264	11	4.1991	0.0145
X267	5	-0.3523	0.0066	X268	11	0.5996	0.0094	X269	11	0.1485	0.0173	X270	23	2.2180	0.0225
X273	11	-1.7410	0.0120	X274	23	1.1915	0.0119	X288	5	4.2431	0.0138	X289	5	-0.9758	0.0094
X290	5	-3.6025	0.0098	X291	11	0.7041	0.0083	X292	11	0.7999	0.0068	X293	23	-0.3417	0.0090
X294	5	-1.3798	0.0134	X295	5	3.6416	0.0140	X298	5	-1.7040	0.0075	X299	5	0.5191	0.0067
X300	11	12.0268	0.0223	X301	23	1.2879	0.0202	X302	23	-1.6356	0.0212	X306	11	-1.9796	0.0095
X307	23	0.5661	0.0067	X308	5	2.0384	0.0093	X309	11	10.0127	0.0245	X310	23	-1.8687	0.0166
X311	11	0.2001	0.0160	X312	23	1.5270	0.0152	X315	11	-0.8510	0.0085	X316	23	0.3150	0.0077
X317	23	-4.7085	0.0185	X318	35	-11.7594	0.0522	X319	35	-1.1479	0.0118	X323	23	0.0986	0.0076
X324	35	2.3411	0.0196	X325	23	0.9085	0.0356	X326	11	-11.7344	0.0539	X327	23	-3.4117	0.0372
X328	11	0.1028	0.0070	X329	23	-0.6780	0.0062	X330	11	-4.7766	0.0207	X331	23	0.6541	0.0198
X332	23	-5.3999	0.0410	X333	23	-12.5433	0.0390	X334	23	-81.8098	0.1516	X335	23	6.5450	0.0174
X336	5	-0.9022	0.0049	X337	11	-0.9572	0.0057	X338	11	-1.7703	0.0094	X339	23	0.6676	0.0079
X340	23	-2.0538	0.0186	X341	23	1.8776	0.0037	X342	23	0.1372	0.0216	X365	5	6.9251	0.0075
X366	11	-0.5526	0.0052	X368	11	1.2622	0.0069	X369	23	-1.5311	0.0078	X374	35	2.1049	0.0080
X375	23	6.0401	0.0106	X380	23	1.4643	0.0055	X382	35	-2.0761	0.0071	X383	5	-4.0400	0.0103
X384	11	1.3371	0.0102	X385	11	-0.7888	0.0066	X386	23	1.3032	0.0094	X387	23	-7.8607	0.0162
X388	23	-0.0936	0.0056	X389	23	-0.5507	0.0127								

- **Statistics of running α^5 code:**
  - $\star$ **10 - 20 minutes for generation of a FORTRAN code for each diagram on DEC α.**
  - $\star$ **Typical integral consists of 90,000 lines of FORTRAN code occupying more than 6 Megabytes.**
  - $\star$ 10^6 **sampling points $\times$ 20 iterations takes 5 - 7 hours on 32 CPU PC cluster.**
- **Step V for residual renormalization is being carried out.**
- **We will soon have a crude value of Set V.**

5. Remaining task

- **Next on schedule is treatment of IR divergence by IR div. subtraction method, which enables us to put $\lambda = 0$.**

- **The method developed for Set V enables us to evaluate Set III(a), Set III(b), and Set IV very quickly.**

- **Sets I(a, b, c, d, e, f), II(a, b, f), VI(a, b, c, e, f, i, j, k) had been evaluated previously.**

  T. Kinoshita and M. Nio, Phys. Rev. D 73, 053007 (2006)

- **Remaining sets I(g, h, i, j), II(c, d, e), III(c), and VI(d, g, h) do not seem to present particular complication except possibly for I(i), I(j), II(e).**

- **We will have a complete α^5 term within few years.**